AD-A078 538 HUGHES RESEARCH LABS MALIBU CA F/G 9/1
OPTICAL-MICROWAVE INTERACTIONS IN SEMICONDUCTOR DEVICES.(U)
OCT 79 L FIGUEROA , C SLAYMAN , H W YEN N00173-78-C-0192
UNCLASSIFIED NL

1 OF 1
AD-
A078538

END
DATE
FILMED
1-80
DDC

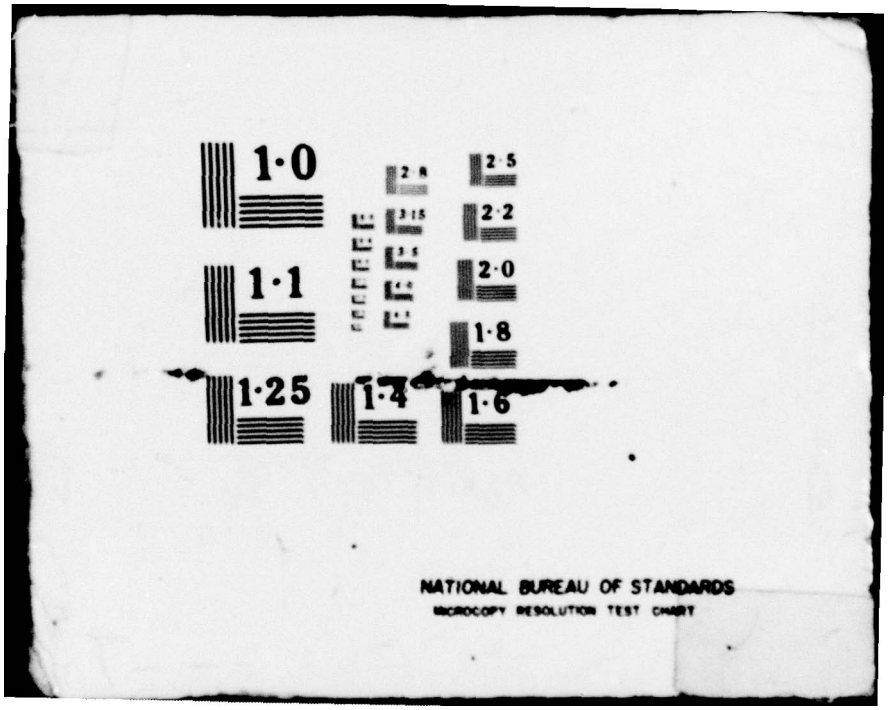
1·0
1·1
1·25
1·4
1·6
2·0
2·2
2·5
NATIONAL BUREAU OF STANDARDS
MICROCOPY RESOLUTION TEST CHART

OPTICAL–MICROWAVE INTERACTIONS IN SEMICONDUCTOR DEVICES

L. Figueroa, C. Slayman, and H.W. Yen

Hughes Research Laboratories
3011 Malibu Canyon Road
Malibu, CA 90265

October 1979

N00173–78–C–0192
Quarterly Report 5
For period 1 July 1979 through 30 September 1979

Approved for public release; distribution unlimited.

Sponsored by
DEFENSE ADVANCED RESEARCH PROJECTS AGENCY
1400 Wilson Boulevard
Arlington, VA 22209

Prepared for
NAVAL RESEARCH LABORATORY
4555 Overlook Avenue, S.W.
Washington, DC 20375

The views and conclusions contained in this document are those of the authors and should not be interpreted as necessarily representing the official policies, either expressed or implied, of the Defense Advanced Research Projects Agency or the U.S. Government.

UNCLASSIFIED

SECURITY CLASSIFICATION OF THIS PAGE (When Data Entered)

REPORT DOCUMENTATION PAGE

READ INSTRUCTIONS BEFORE COMPLETING FORM

1. REPORT NUMBER

2. GOVT ACCESSION NO.

3. RECIPIENT'S CATALOG NUMBER

4. TITLE (and Subtitle)

OPTICAL-MICROWAVE INTERACTIONS IN SEMICONDUCTOR DEVICES

5. TYPE OF REPORT & PERIOD COVERED

Quarterly Report
1 July 1979 — 30 Sept 1979

6. PERFORMING ORG. REPORT NUMBER

7. AUTHOR(s)

L. Figueroa, C. Slayman, and H.W. Yen

8. CONTRACT OR GRANT NUMBER(s)

N00173-78-C-0192

9. PERFORMING ORGANIZATION NAME AND ADDRESS

Hughes Research Laboratories
3011 Malibu Canyon Road
Malibu, CA 90265

10. PROGRAM ELEMENT, PROJECT, TASK AREA & WORK UNIT NUMBERS

11. CONTROLLING OFFICE NAME AND ADDRESS

Defense Advanced Research Projects Agency
1400 Wilson Boulevard
Arlington, VA 22209

12. REPORT DATE

11 October 1979

13. NUMBER OF PAGES

29

14. MONITORING AGENCY NAME & ADDRESS (if different from Controlling Office)

Naval Research Laboratory
4555 Overlook Ave., S.W.
Washington, DC 20375

15. SECURITY CLASS. (of this report)

UNCLASSIFIED

15a. DECLASSIFICATION DOWNGRADING SCHEDULE

16. DISTRIBUTION STATEMENT (of this Report)

Approved for public release; distribution unlimited.

17. DISTRIBUTION STATEMENT (of the abstract entered in Block 20, if different from Report)

18. SUPPLEMENTARY NOTES

19. KEY WORDS (Continue on reverse side if necessary and identify by block number)

GaAs FETs, GaAs Gunn diodes, GaAs FET detector, liquid phase epitaxial crystal growth, optical waveguide.

20. ABSTRACT (Continue on reverse side if necessary and identify by block number)

GaAs FETs and Gunn diodes with built-in optical waveguides are being developed. The purpose is to allow optical signals to be coupled into the active region of the devices efficiently. These FETs will be useful for optical mixing, optical injection locking, and optical detection purposes. The Gunn diodes will be used for high-speed pulsed modulation of injection lasers.

DD FORM 1 JAN 73 1473 EDITION OF 1 NOV 65 IS OBSOLETE

UNCLASSIFIED

SECURITY CLASSIFICATION OF THIS PAGE (When Data Entered)

172600

We have designed and fabricated a novel FET configuration. The structure consists of three layers: a GaAs active layer, a $Ga_{0.6}Al_{0.4}As$ waveguide layer, and a $Ga_{0.55}Al_{0.45}As$ buffer layer. The waveguide layer is made into a strip-loaded channel guide which serves as the input port for the optical signal. The guided optical signal leaks into the GaAs active layer once it reaches the FET mesa structure and is absorbed. Preliminary results indicated that side illumination using such a device can generate more photocurrent than top illumination. The frequency response of the device as an optical detector was measured. For a 10-μm-long device, the measured 3-dB cutoff frequency is about 1.4 GHz.

TABLE OF CONTENTS

LIST OF ILLUSTRATIONS

PREFACE

The following personnel contributed to the research work reported here: L. Figueroa, C. Slayman, H.W. Yen, and D.F. Lewis.

SECTION 1

INTRODUCTION AND SUMMARY

The ability to control the frequency and phase of solid-state microwave oscillators by optical injection of modulated light will allow optical fiber waveguides to replace heavy metallic waveguides in many microwave communication and radar applications. To realize this replacement, we require microwave-modulated optical sources, as well as a new class of microwave devices capable of interacting strongly with modulated optical signals.

The purpose of this study is to develop unique hybrid optical-microwave devices with optimal optical-microwave interaction characteristics. Specifically, we are developing GaAs FETs and GaAs Gunn diodes with built-in optical waveguides so that optical signals can be coupled to the active region of the device efficiently. The FETs will be used for optical mixing, optical injection locking, and optical detection purposes. The Gunn diodes will be used for high-speed pulse modulation of injection lasers.

During this quarter, we continued with the fabrication and characterization of GaAs FETs and Gunn diodes. The structure of the GaAs FETs from the initial runs consisted of two layers: the GaAs channel layer and the $Ga_{0.6}Al_{0.4}As$ low doping layer. The source-drain current versus source-drain voltage characteristics of these devices showed peculiar behavior depending on whether or not optical illumination was present. This seems to be a problem associated with defects at the interface or at the Schottky gate. The problem was eliminated in subsequent runs. GaAs Gunn diodes were fabricated with a two-layer structure similar to that used for FETs. Devices with different length and thickness were fabricated to investigate their effects on device efficiency.

A novel FET configuration was designed and fabricated. The structure consists of three layers: the GaAs top layer, the $Ga_{0.6}Al_{0.4}As$ waveguide layer, and the $Ga_{0.55}Al_{0.45}As$ buffer layer. The waveguide layer is made into a strip-loaded channel guide and serves as the input port for the optical signal. The guided optical signal will leak into the GaAs layer once it reaches the FET mesa structure and will be absorbed there. Preliminary results indicated that side illumination using such a device can generate more photocurrent than can top illumination. The frequency response of the device as an optical detector was measured. For a 10-μm-long device, the measured 3-dB cutoff frequency is about 1.4 GHz.

SECTION 2

DEVICE FABRICATION AND CHARACTERIZATION

In our last quarterly report, we proposed a modified GaAs FET structure that we felt should improve the coupling efficiency of light into the device. During this period, we fabricated such a device. It is fabricated by starting with a piece of Cr-doped GaAs semi-insulating substrate and growing successively an n-$Ga_{0.6}Al_{0.4}As$ (~5 μm) layer and an n-GaAs (~1 μm) layer. The GaAs layer is the active region of the FET, and the $Ga_{0.6}Al_{0.4}As$ layer acts as a buffer layer.

After the layers are grown, three masks are used in the photolithographic process to fabricate the FETs. The first mask is used to define a square GaAs active mesa so that current leakage around the gate in the GaAs layer is minimized. The second mask defines the source and drain electrodes using the lift-off technique. The third mask defines the gate electrode, also by the lift-off technique.

Figure 1 shows the dc characteristics of one of the early devices. It shows the source-drain current as a function of the source-drain voltage with the gate voltage as a parameter. Figure 1(a) is for the case when the microscope illuminating light is turned off. It is interesting to note the bunching of some of the curves. Figure 1(b) shows what happens when the light is turned on. The peak source-drain current increases slightly while at the same time the curves for various values of gate voltages are more or less evenly spaced. Thus it appears that optical illumination in this case actually improves the FET characteristics. We believe that either the Schottky gate or the GaAs-$Ga_{0.6}Al_{0.4}As$ interface of the device is imperfect. If this is true, then the defects or the traps are responsible for the poor characteristics. Optical illumination can excite extra charge carriers and fill up the traps, hence normal FET characteristics are obtained.

9253-12

(a)

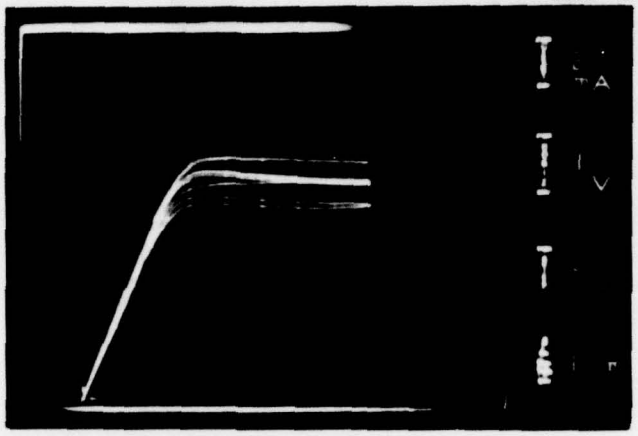

(b)

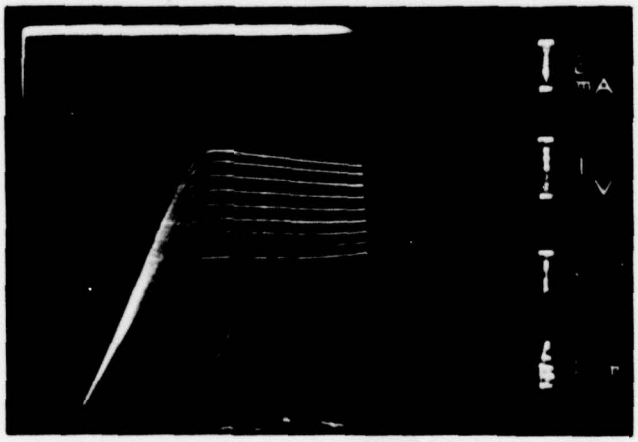

Figure 1. GaAs FET characteristics
(a) without illumination,
(b) with illumination.

In our later runs, as Figure 2 shows, the devices did not show the peculiar response observed earlier. It is clear from both Figures 1 and 2 that our FETs could not, because of the thick active layer used, be pinched-off. One can calculate the pinch-off voltage V_p of an FET using the formula:[1]

$$V_p = \frac{eNd^2}{2\varepsilon\varepsilon_o},$$

where e is the electronic charge, N is the channel layer doping concentration, d is the channel layer thickness, ε is the dielectric constant of GaAs, and ε_o is the permittivity of free space. For $N = 7.0\times10^{16}/cm^3$ and $\varepsilon = 12.3$, we have $V_p = 51.4$ V for $d = 1$ μm, and $V_p = 12.9$ V for $d = 0.5$ μm. Since the pinch-off voltage is proportional to the square of the layer thickness, it is important to control the active layer thickness precisely.

To enhance the interaction between the optical beam and the Gunn domain in a Gunn diode, we propose using a wave-guiding structure in the vertical direction, as shown in Figure 3. Several Gunn diodes were fabricated with four different lengths: 30 μm, 60 μm, 80 μm, and 130 μm. Figure 4 gives a series of curve-tracer photographs showing the current-voltage (I-V) characteristics of Gunn diodes of various lengths. The horizontal scale is 2 V per division, and the vertical scale is 10 mA per division. Figure 4(a) is for a sample 130 μm long. The saturation current level of the device is ~44 mA at a bias level of ~14 V. There appears to be current oscillation for bias voltages larger than 17 V. Figure 4(b) is for a device 80 μm long. The saturation current is ~49 mA, and the corresponding voltage is ~10 V. Again, there appears to be current oscillation in the device at large bias. Figure 4(c) is for a device 60 μm long. The saturation current increases to ~54 mA under a bias of ~7.5 V. Figure 4(d) is for a device 30 μm long. The saturation voltage is less than 6 V, and the

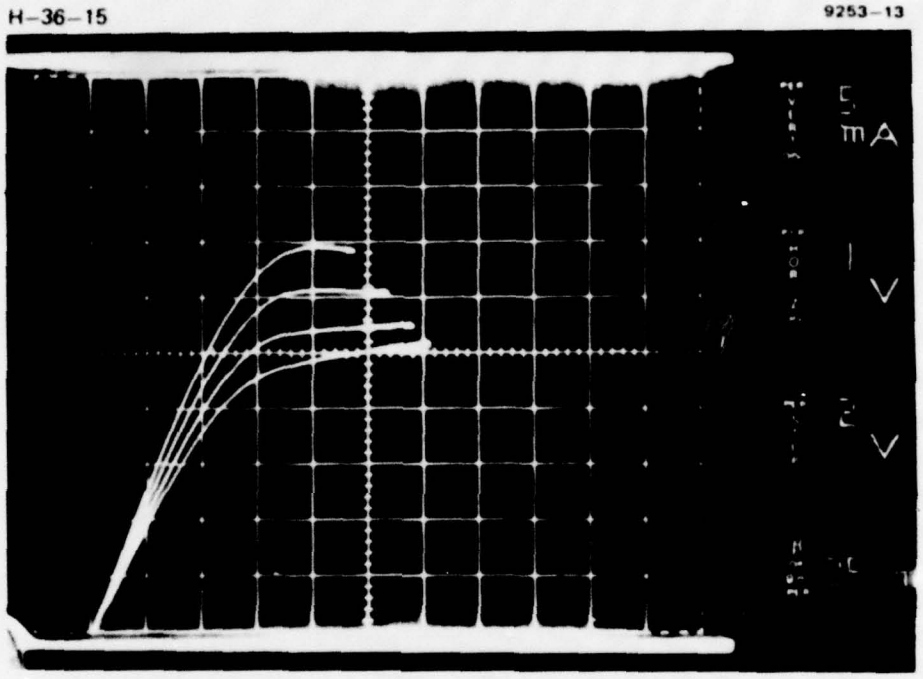

Figure 2. Improved GaAs FET characteristics.

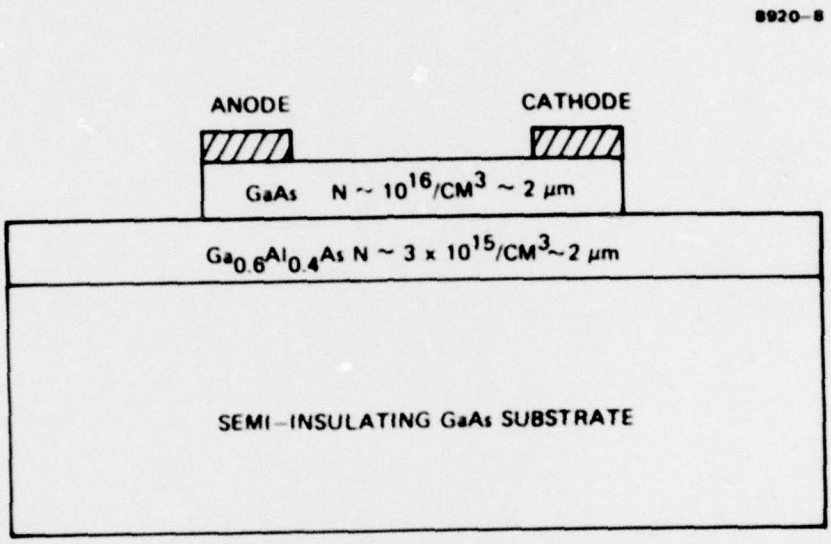

Figure 3. Cross section of a Gunn diode with optical waveguiding structure.

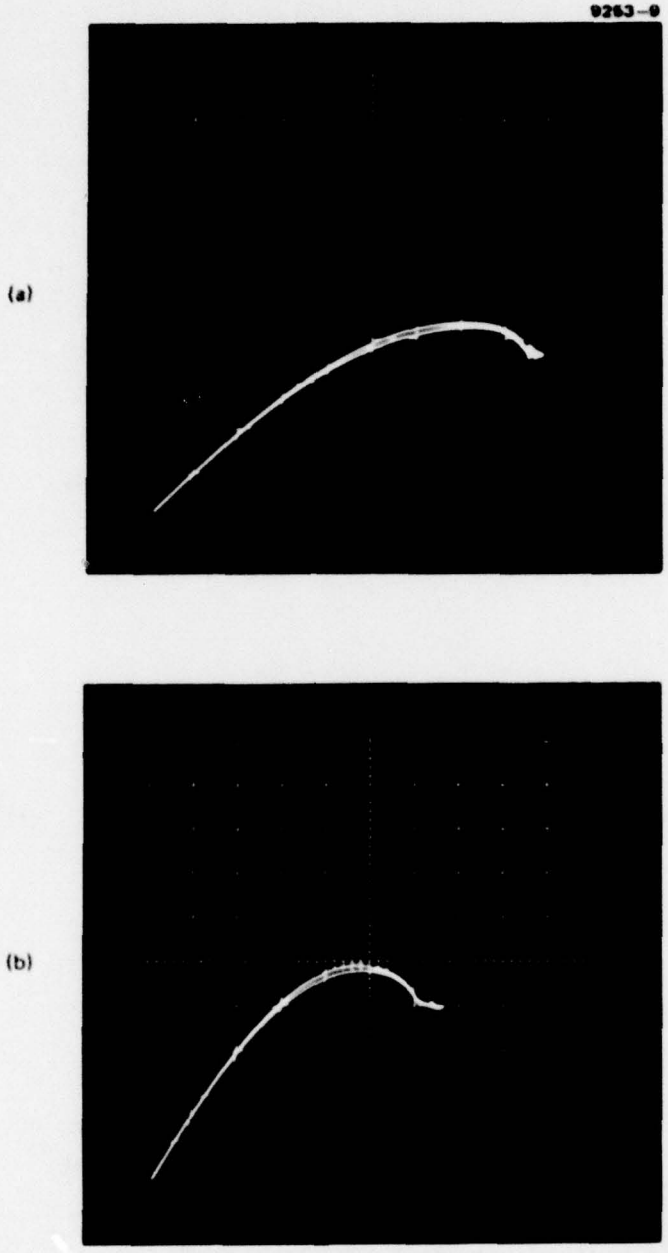

Figure 4. I-V curves of Gunn diodes of various lengths (L). Vertical scale is 10 mA/div, horizontal scale is 2 V/div. (a) L = 130 μm, (b) L = 80 μm.

9253-8

(c)

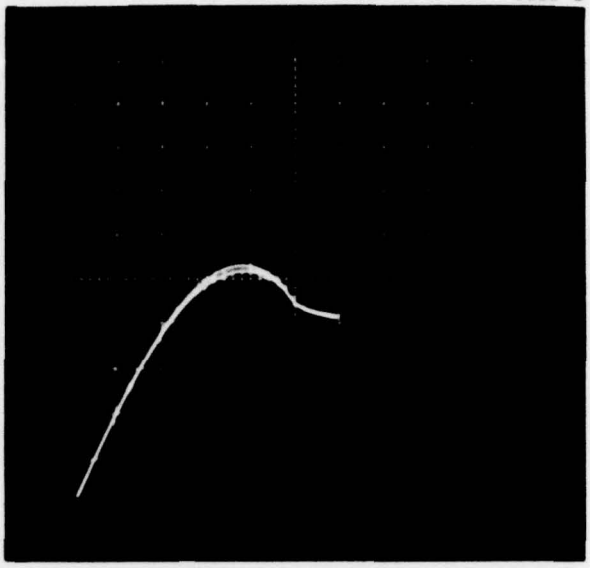

(d)

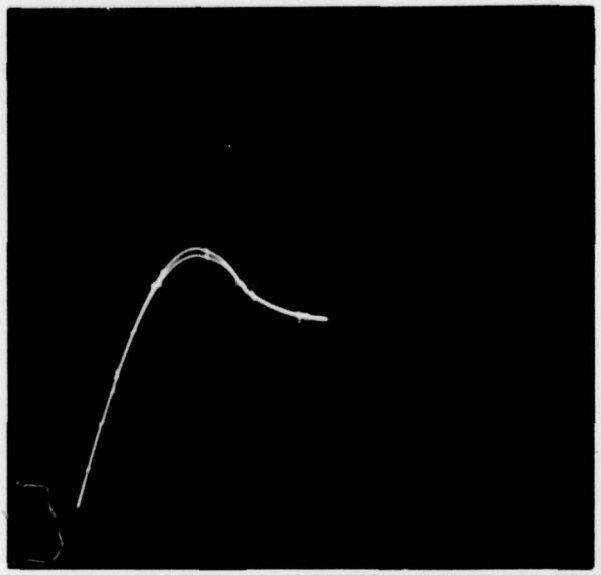

Figure 4 (continued). (c) L = 60 μm, (d) L = 30 μm.

current is 57 mA. The general trend of this series of devices is that the saturation current level is inversely proportional to the device length and the critical voltage is proportional to the device length. Also, the amount of current drop beyond the critical voltage of the device seems to increase for shorter devices.

SECTION 3

GaAs FET WAVEGUIDE DETECTOR

In the last quarterly report, we discussed the use of a GaAs FET as an optical detector. Initially, we suggested using a "Burrus-type structure" such as shown in Figure 5. But during the fabrication of the FETs, we found that our mask aligner tended to break thin GaAs substrates during contact exposures. This problem led us to decide against pursuing the "Burrus structure," at least for now. Instead, we conceived a novel waveguide FET configuration that is capable of high-speed detection and can be easily integrated with FET amplifiers or other integrated optical components. This section describes some preliminary experimental results.

A cross section and a top view of the finished device are shown in Figure 6. The device consists of three layers: $Ga_{0.55}Al_{0.45}As$ ($N \simeq 3x10^{15}/cm^3$), $Ga_{0.6}Al_{0.4}As$ ($N \simeq 3x10^{15}/cm^3$), and GaAs ($N \simeq 1x10^{17}/cm^3$) grown by liquid-phase epitaxy. The thickness of the layers are 3.1 μm, 1.9 μm, and 1 μm, respectively.

After the layers have been grown, a GaAs mesa is defined by selective chemical etching and a 5-μm-wide, strip-loaded waveguide, which is aligned with the gate electrode of the FET, is formed. The strip loading is accomplished by leaving a thin layer of GaAs oxide over the $Ga_{0.6}Al_{0.4}As$ layer. The FET electrodes are defined as before.

After the electrodes have been formed, the substrate is lapped down to ~100 μm, and individual FET waveguide detectors are cleaved. Typical FETs have a maximum drain-source current of approximately 40 to 60 mA and a transconductance of approximately 2 to $5x10^{-3}$ mho. As shown in Figure 6(b), the structure consists of a strip-loaded waveguide, which guides the input light under the gate of the FET. Since the index of refraction of $Ga_{0.6}Al_{0.4}As$ ($n = 3.2$) is lower than that of GaAs ($n = 3.6$), the light is coupled into the FET active region and

8567-3a

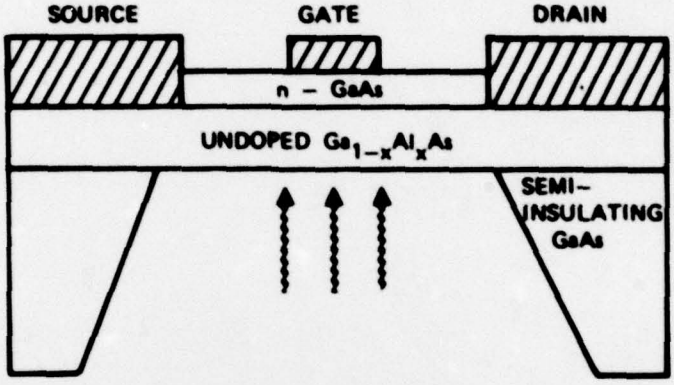

Figure 5. Modified GaAs FET structure with back-illumination access.

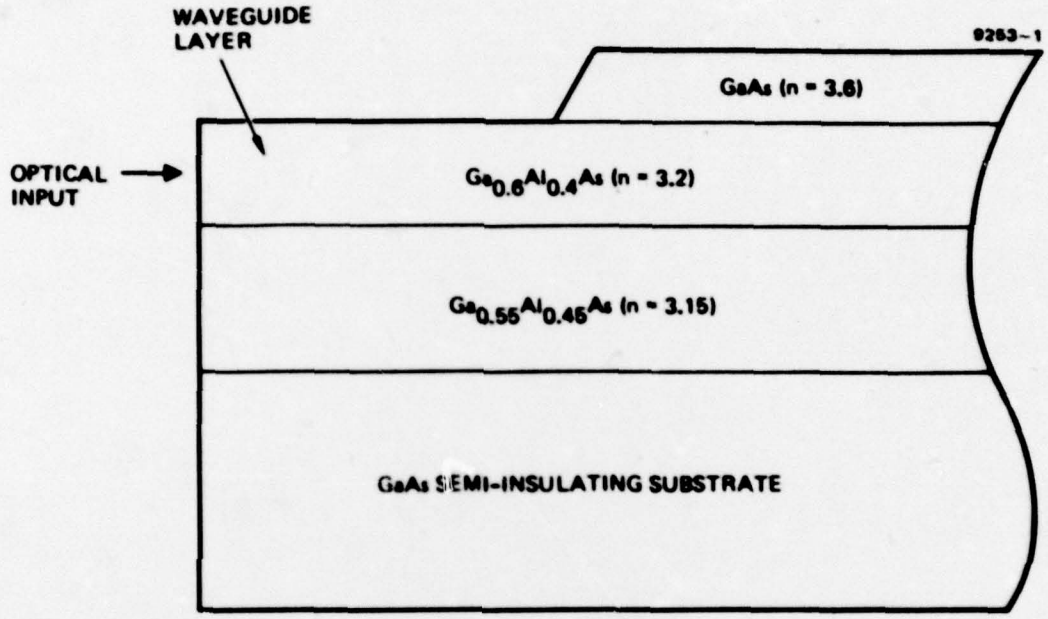

Figure 6(a). Cross section of the waveguide FET detector.

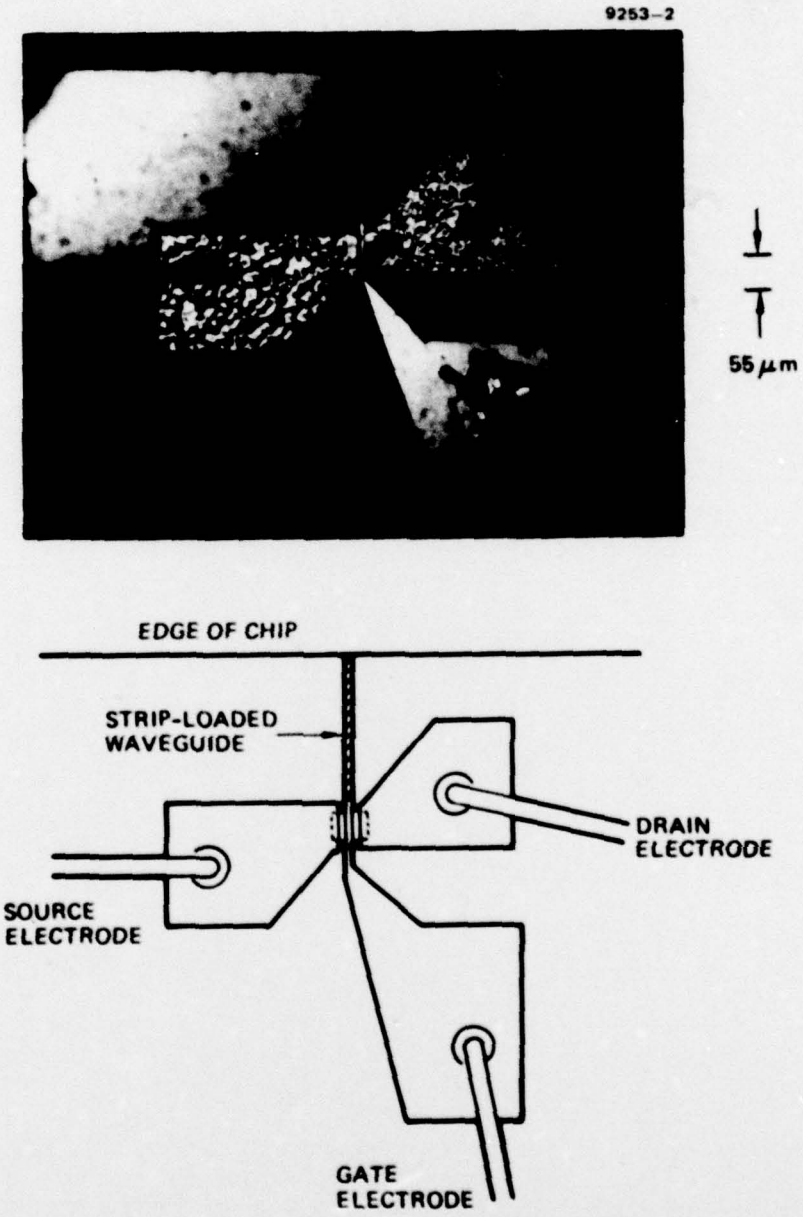

Figure 6(b). Top view of the waveguide FET detector.

generates carriers that in turn produce a photo-current. This detector can operate in the wavelength region of 0.64 μm to 0.9 μm. A similar scheme was used to couple light from a Ti-diffused $LiNbO_3$ waveguide into a silicon p-n junction detector.[2] However, in the scheme presented here, we have monolithically integrated the waveguide and the detector. This will significantly increase the coupling efficiency between the detector and the guided optical signals.

We have made preliminary measurements of both the dc and rf responses of the detector. The experimental circuits used are shown in Figure 7. Figure 8 shows the characteristics of the GaAlAs laser used for the light source. The output from the laser is focused onto the detector using a 20X microscope objective. Figure 9 shows plots of the detected photocurrent versus laser injection current for two FET orientations. Side illumination is accomplished by focusing the light into the strip-loaded waveguide, while top illumination is achieved by shining the light between the metal contacts. The results of these two illumination schemes are quite different.

The photocurrent generated by side illumination appears to follow the laser power versus current curve closely. But the current due to top illumination appears to saturate. Figure 10 shows the effect of drain-to-source voltage on the detector photocurrent. The curve has two distinct regions: a saturation region corresponding to carrier velocity saturation, and a linear region corresponding to a linear relationship between the carrier velocity and the electric field.

Figure 11 shows the measured frequency response of the FET detector. The measurement was performed by modulating the injection laser using a microwave sweep oscillator. The output of the detector was fed into an amplifier with ~30 dB gain; its output was connected to a spectrum analyzer, from which the magnitude of the detected frequency component was then read off. The frequency response data of the detector was corrected for variations in the sweep oscillator output, but no

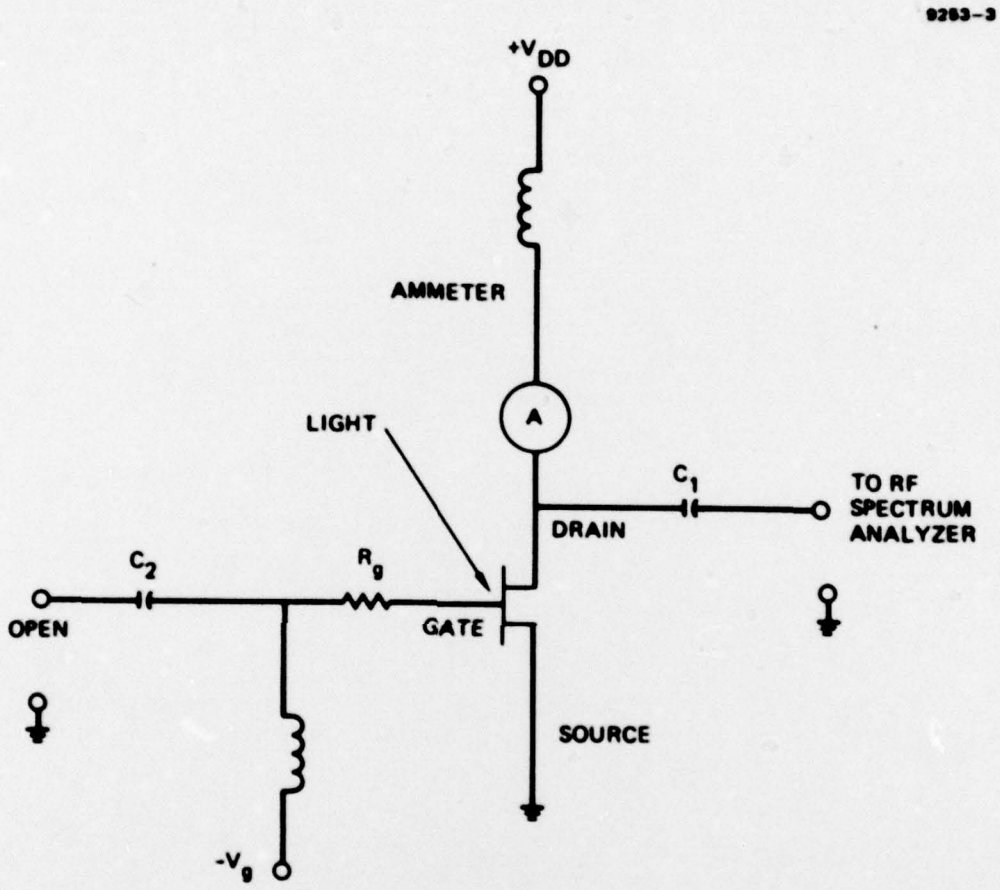

Figure 7. Circuits used for characterizing GaAs FET waveguide detector.

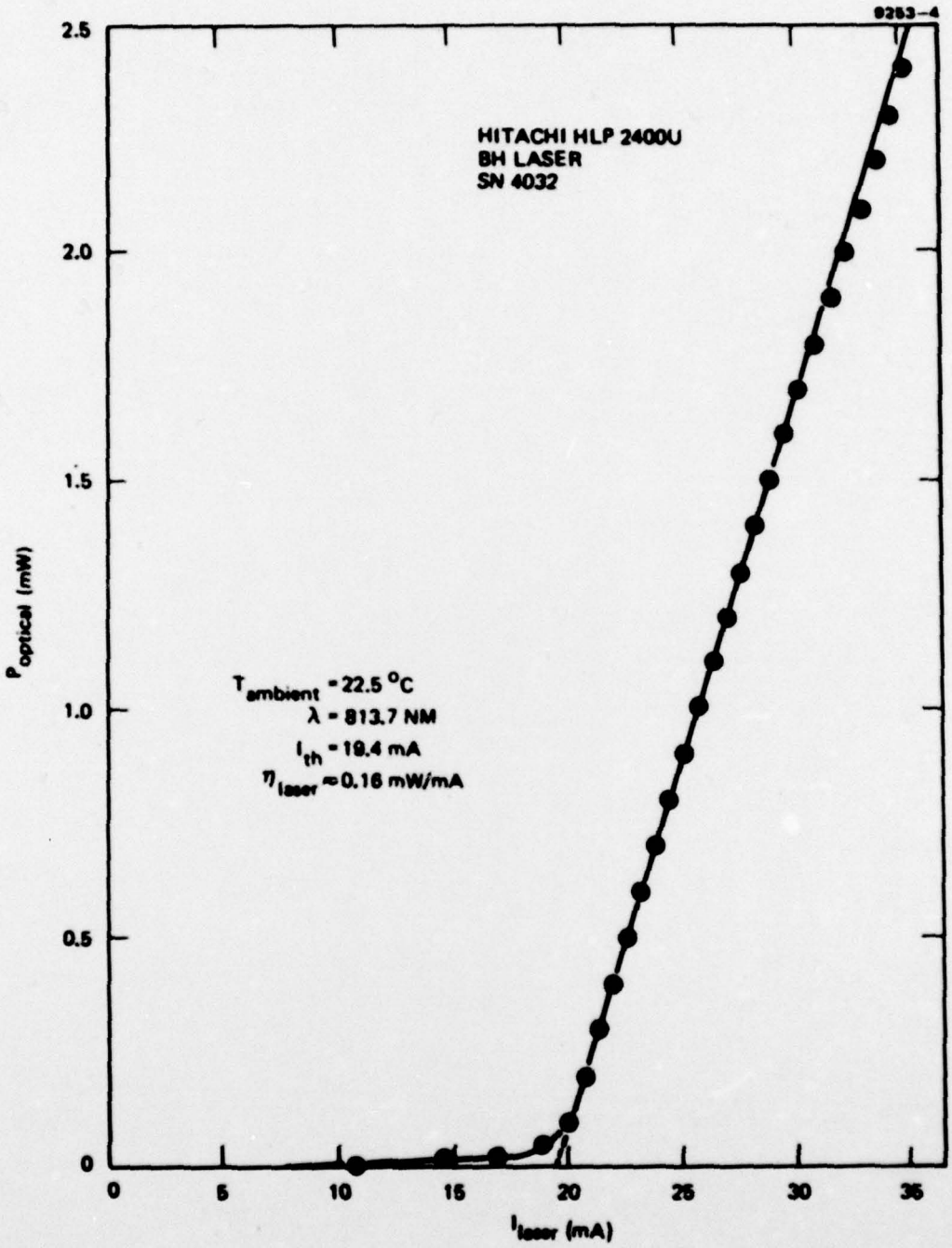

Figure 8. Power versus current for the injection laser used in the experiment.

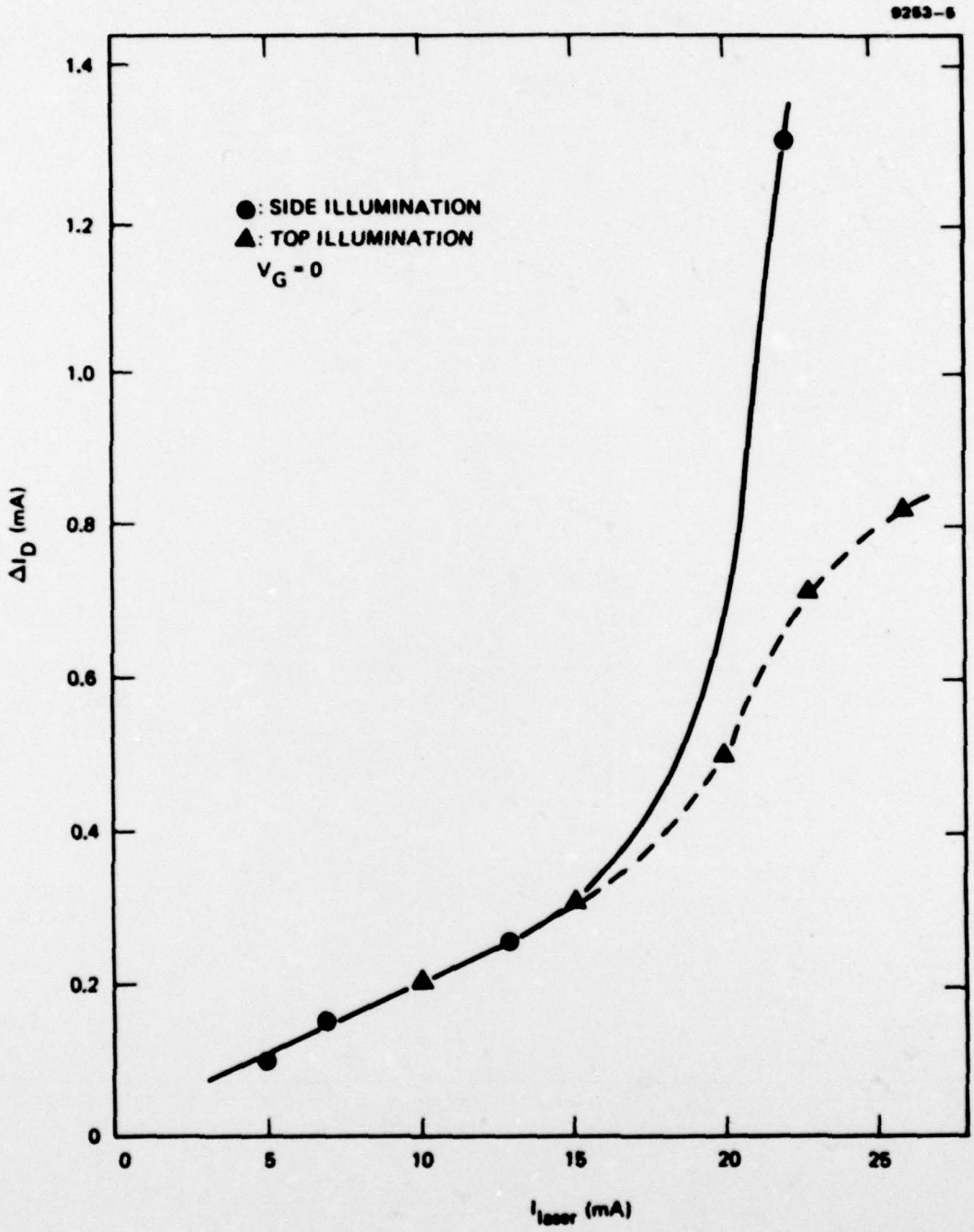

Figure 9. DC photocurrent of the FET detector as a function of the drive current of the light source.

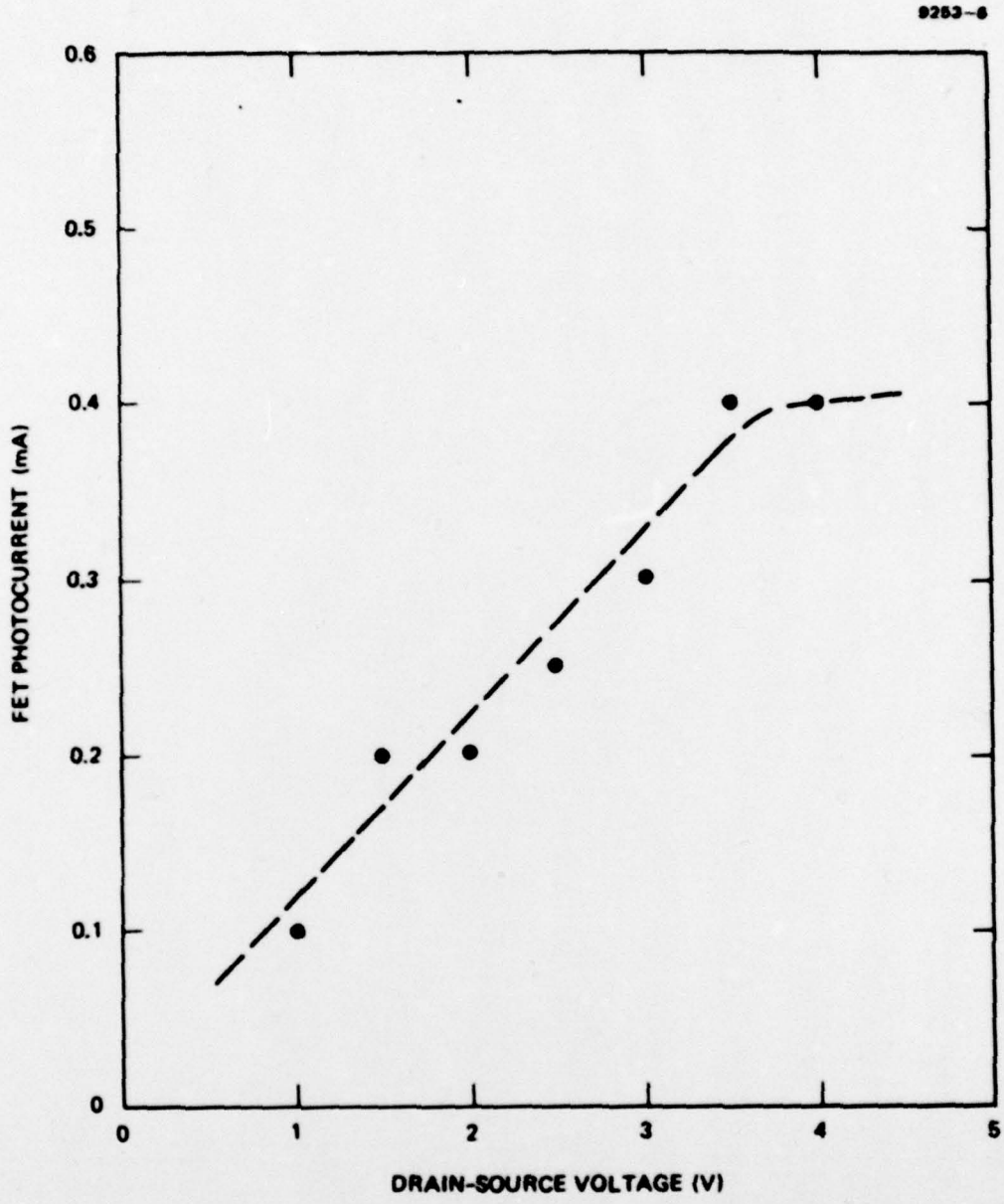

Figure 10. FET photocurrent versus drain-source voltage with no gate bias.

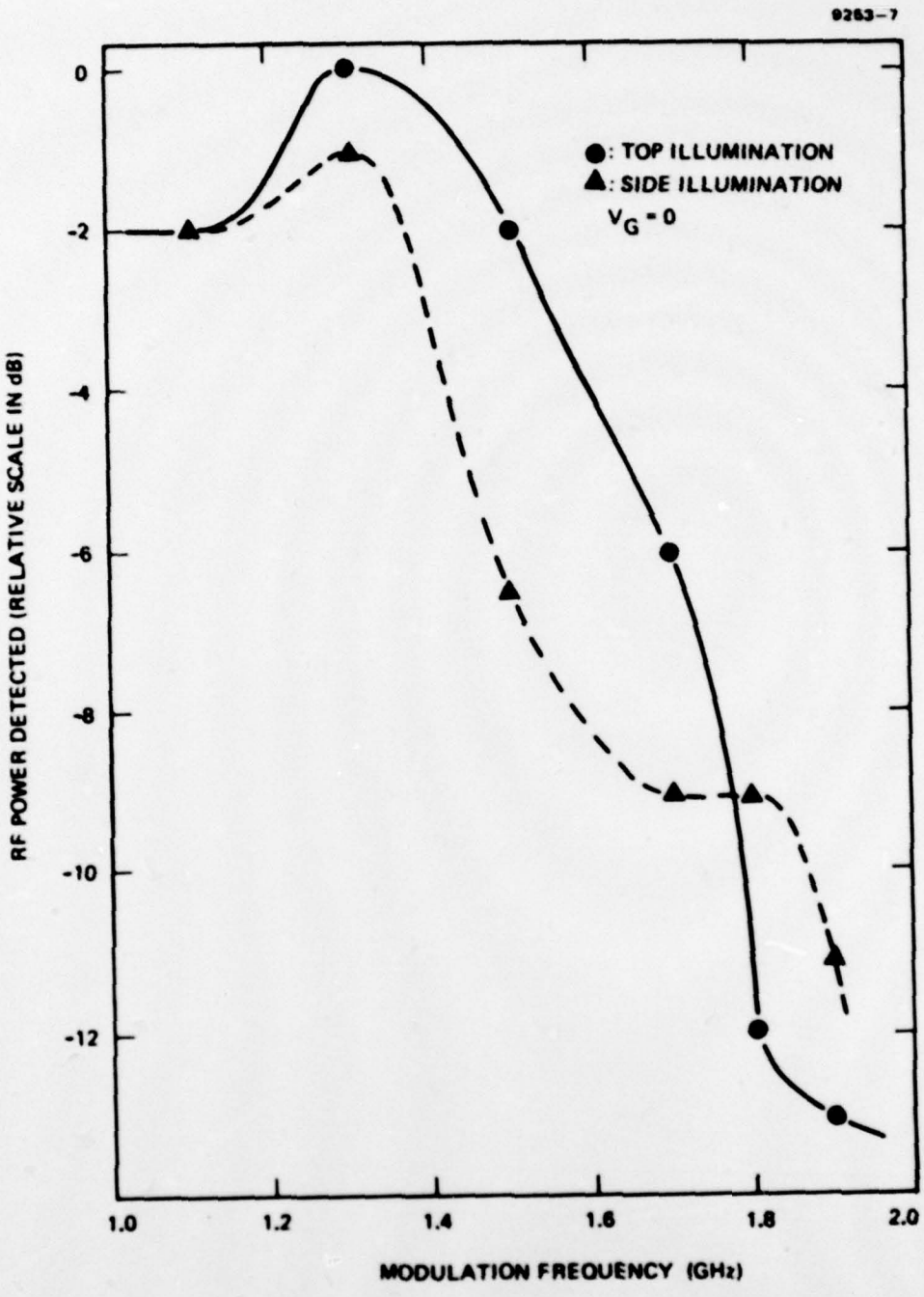

Figure 11. Frequency response of a GaAs FET detector.

attempt was made to correct for the laser frequency response. (The laser is expected to have a fairly flat frequency response up to ~2 GHz at the drive level used ($I \sim 1.25\ I_{th}$).) Figure 11 shows that the FET detector can respond to gigahertz modulation rates. The 3-dB cutoff frequency measured for the device is ~1.4 GHz.

The photocurrent generated in a photoconductive detector can be expressed as[3]

$$i_d = \frac{e\eta P}{h\nu}\left(\frac{\tau_o}{\tau_d}\right), \tag{1}$$

where e is the electronic charge, η is the quantum efficiency, P is the incident optical power, $h\nu$ is the energy carried by each individual photon, τ_o is the lifetime of excess carriers, and τ_d is the transit time of the carriers. The small-signal frequency response of a photoconductive detector is given by[4]

$$i_d(\omega) = \frac{e\eta P}{h\nu}\left(\frac{\tau_o}{\tau_d}\right)\frac{1}{\left[1 + (\omega\tau_o)^2\right]^{\frac{1}{2}}}.$$

Therefore, the 3-dB cutoff frequency of such a detector is

$$f = \frac{1}{2\pi\tau_o}.$$

Using the results from Figure 11, we find that $\tau_o \simeq 114$ psec, which is in rough agreement with values measured by others. This lifetime is primarily due to surface rather than bulk recombination: bulk recombination time is about 1 nsec. Using Eq. 1 and Figure 9, we can estimate the optical power coupled into the FET detector to be ~0.11 mW. This corresponds to ~28% of the light emitted by the laser (Figure 8). Thus, the coupling efficiency of the waveguide FET is reasonably high.

SECTION 4

PLANS FOR THE NEXT QUARTER

In the next quarter, we will continue the study of modified GaAs FETs. More devices will be fabricated with thinner active layers so that the FET can be pinched-off with reasonable gate bias voltages. We will characterize the FETs as high-speed optical detectors with particular emphasis on the effect of gate bias on the photocurrent. GaAs Gunn diodes will be mounted in appropriate circuits so that domains can be generated in the diodes for the optical modulation experiments.

REFERENCES

1. S.M. Sze, Physics of Semiconductor Devices, New York; Wiley, 1969.

2. T.R. Ranganath and S. Wang, Appl. Phys. Lett., 31, 803 (1977).

3. A. Yariv, Introduction to Optical Electronics, New York; Holt, Rinehart and Winston, 1971.

4. M. DiDomenico, Jr., and O. Svelto, Proceedings of IEEE, 52, 136 (1964).